A Robust Method for the Estimation of 4D Pharmacokinetic Parameters in dceMRI Data in Colorectal Cancer Patients

*Darren Morofke[a], E. Mark Anderson [b], Fergus V. Gleeson[b], Sir Michael Brady[a]

[a] Wolfson Medical Vision Laboratory, Department of Engineering Science, University of Oxford, UK, [b] Department of Radiology, Oxford Radcliffe Hospitals, UK

Abstract. To date, most clinical studies of colorectal cancer patients have used only one or, more recently, two image slices through a tumour. This has largely been due to technological limitations in MRI scanners and to practical computational limits. Using high-speed multi-coil MRI machines, we have been able to capture and analyze full 4D datasets acquired from dceMRI on 20 human colorectal cancer patients with over 50 slices per patient of visualization. To analyze this data, we have created software for data capture and automated analysis. We compare our techniques and results to existing methods.

1 Introduction and clinical procedure

Colorectal cancer survival has doubled in the past 30 years, largely due to advances in screening and early detection methods, nevertheless in the UK alone 16,000 people die of the disease each year. We have completed a clinical trial with 20 patients, obtaining 4-dimensional (4D) dynamic contrast enhanced (dce) MRI scans using a GE Signa HD 1.5T multi-coil scanner. Our patients underwent a typical clinical scans followed by two research protocols and was ethically approved by CORREC. Presented here is the methodology used to analyse our data.

It has been shown [1] that contrast agent uptake has a non-linear effect on signal enhancement, the nonlinearity being related to native T_1 values. Thus the first protocol was a 3D native T_1 mapping sequence. A 4D multi-coil volumetric sequence, LAVA, followed with a temporal resolution of 12-15s per volume and a spatial resolution of 0.78x0.78x2mm. After 5 temporal volumes were captured with the LAVA sequence, the auto-injector was used to inject Gd(HP-DO3A), or ProHance, intravenously. The initial uptake and wash out of the contrast agent was recorded over a period of 5-7 minutes using the 5 pre-contrast agent scans as a baseline image. Data was fitted on a voxel-by-voxel basis, for all voxels with a T_1 value greater than 350mS. Furthermore, T_1 estimation was capped at 2000mS to counter sub-voxel motion causing errors in estimation.

2 Methodology

2.1 Optimal filtering for noise removal

Rapid acquisition times for MRI volumes comes at the price of noise artefacts. Such artefacts can have a significant impact on subsequent estimation, so it is important to automatically and accurately remove or smooth out noise. In cancer imaging, the edges of the tumour are a major determining factor for classification of the cancer stage. Anisotropic filtering is one technique that smooths an image while preserving edges, and fast implementations are available in ITK and MATITK [2]. A modified curvature diffusion equation (MCDE) anisotropic filter can avoid the edge enhancing properties that are inherent in classic anisotropic diffusion. This is calculated as,

$$ft = |\nabla f| \nabla \cdot c(|\nabla f|) \frac{\nabla f}{|\nabla f|}, \tag{1}$$

2.2 Estimate T_1 values

Using a fast-spoiled gradient echo sequence (FSPGR), the native T_1 values can be estimated accurately and quickly (~5 minutes of MRI scanner time) for a large volume. The intensity of a FSPGR signal intensity at each voxel is represented as:

$$S_{SPGR} = g\rho e^{-\frac{TE}{T_2^*}} \frac{\left(1 - e^{-\frac{T_R}{T_1}}\right)\sin\alpha}{1 - e^{-\frac{T_R}{T_1}}\cos\alpha}, \tag{2}$$

* Corresponding author, Darren . Morofke (at) eng. ox. ac. uk.

where S is the observed signal intensity, g is the scanner gain, ρ is the proton density, T_E is the echo time, T_1 / $T2^*$ is the longitudinal / transverse relaxation time, T_R is the repetition time, and α is the flip angle. By holding T_R constant, the flip angle and signal intensity together become dependent values. This linear relationship can be estimated as,

$$\frac{S_{SPGR}}{\sin\alpha} = e^{-\frac{T_R}{T_1}}\frac{S_{SPGR}}{\tan\alpha} + M_0\left(1-e^{-\frac{T_R}{T_1}}\right),\ T_1 = -\frac{T_R}{\ln(m)},\quad M_0 = \frac{b}{1-m}, \tag{3, 4,5}$$

where M_0 is a constant encompassing proton density, gain and the transverse relaxation time, and m and b are the slope and intercept of equation 3.

2.3 T_1 estimation without holding T_R constant

If T_R cannot be held constant between scans, equations 3-5 are no longer valid. However, it follows from equation 2 that the change in T_R will manifest itself in a predictable change in intensity. The change in signal intensity between two images can be predicted by,

$$S_1 = \frac{\left(1-e^{-\frac{T_{R1}}{T_1}}\right)\left(1-e^{-\frac{T_{R2}}{T_1}}\cos\alpha\right)}{\left(1-e^{-\frac{T_{R1}}{T_1}}{}_1\cos\alpha\right)\left(1-e^{-\frac{T_{R2}}{T_1}}\right)}S_2, \tag{6}$$

where S_1/S_2 is the adjusted/original signal intensity, T_{R1}/T_{R2} is the new/old repetition time. This requires prior knowledge of the native T_1 value of each voxel. This problem can be approached iteratively, by creating an initial guess at the T_1 by making the assumption that T_R is equal and using equation 3. By using this value to change the intensity of the image, an iterative loop occurs which converges on a fixed point.

2.4 Estimation of contrast agent concentration

Following injection of a contrast agent such as Gd(HP-DO3A), the transverse and relaxation times change:

$$\frac{1}{T_1} = \frac{1}{T_{10}} + R_1C(t), \frac{1}{T_2^*} = \frac{1}{T_{20}^*} + R_2C(t), \tag{7}$$

where T_{10} and T_{20} are the pre-contrast agent relaxation times, $C(t)$ is the contrast agent at the given time, and R_1=4.5s^{-1}mM^{-1} and R_2=5.5s^{-1}mM^{-1} [4]. By substituting these into equation 2 one can relate signal to contrast uptake as, and an enhancement ratio for the concentration of contrast agent can then be calculated as,

$$\frac{S(T)}{S(0)} - 1 = e^{-R_2C(t)T_E}\left[\frac{1-e^{-P-Q}-\cos\alpha\left(e^{-P}-e^{-2P-Q}\right)}{1-e^{-P}-\cos\alpha\left(e^{-P}-e^{-2P-Q}\right)}\right] - 1, \tag{8}$$

where $P = T_R/T_1$ and $Q = R_1C(t)T_R$. This equation can be solved using a modified Newton-Raphson method with bisection technique or, as shown by Lo [5], approximated using a second order polynomial. By performing a 1st order Taylor these values can then be substituted into equation 8, which can then be formulated as a quadratic function,

$$\left[\begin{array}{l} e^{-P}MN\left(e^{-P}\cos\alpha - 1\right)S(0)\,C(t)^2 + \\ \qquad \left[\left(e^{-P}M - N\left(1-e^{-P}\cos\alpha\right)\right)S(0) - e^{-P}M\cos\alpha(1-e^{-P})S(t)\right]C(t)) + \\ \qquad (1-e^{-P})(1-e^{-P}\cos\alpha)(S(0)-S(t)) = 0 \end{array}\right], \tag{9}$$

where $M=R_1T_R$ and $N = R_2T_E$, which is solved for each time point, $C(t)$, by completing the square.

2.5 PK Modelling

As noted above, rapid MRI acquisition comes at the price of increased noise. Using a gating method, common in Doppler Ultrasound, a floating average can be taken. While this reduces the spatial resolution, it increases its immunity to intermittent noise. This is calculated after the estimation of contrast agent by,

$$\hat{C}_t(t) = \frac{1}{MN}\sum_{m=0}^{M}\sum_{n=0}^{N} C_t(m,n), \tag{10}$$

where M,N are the gate size and m,n are the location in the gate. PK models are also very sensitive to variations in time of initial uptake. In our data, it was found that this did not always occur at the time point immediately following injection. This can be due to factors such as injector delay, human error, or physiological factors such as low blood pressure or cholesterol. Thus, it becomes important to determine locus of uptake prior to fitting a pharmacokinetic model to the TAC. A Levenberg–Marquardt algorithm can then be applied to fit a model to this data. For example, the basic model that we used to fit our data was represented either in generic form [1], and/or by Tofts [6] by,

$$C_t(t) = \frac{A}{a-b}\left(e^{-bt} - e^{-at}\right), \; C_t(t) = \frac{Dv_e K^{trans}}{V_p\left(K^{trans} - k_{out}v_e\right)}\left[e^{-k_{out}t} - e^{\left(-\frac{K^{trans}}{v_e}t\right)}\right], \tag{11, 12}$$

respectively where, A, a and b are the generic model values, and K^{trans}, v_e, V_p, k_{out} are transfer coefficients between the endothelial extravascular space into and out of the plasma compartment. A Delaunay triangulation was performed on the fit versus measured data sets to detect outliers, which are deleted prior to model refitting. This process continues until the fit parameters of the curve do not change significantly. Because the initial uptake of the contrast agent is the determining factor in K^{trans}, the first 4 points of the TAC are not involved in the outlier search.

3 Results

3.1 T_1 estimation with out matched T_R

Our clinical T_1 mapping sequence were performed using four different flip angles (15°, 12°, 9°, 3°). When using a non-specific T_1 mapping FSGPR sequence, we were unable to hold T_E/T_R constant across all the four flip angles. What occurred commonly was that the 15° and 12° flip angles were constant and while the 9° and 3° flip angles had a T_R which while constant with each other varied up to as much as 2mS from the large flip angles. To test our recovery methodology we created simulated data using equation 2 where the large base pair (15°/12°) images were generated with a T_R of 4.5ms while the low base pair (9°/3°) were generated using a T_R ranging from 2.5ms to 6.5ms. Our recover method converged within 3 iterations to 1% of the original T_1 used for the generation of these data points. Using MATLAB, 3 iterations took 0.2ms per voxel, demonstrating that this is a computationally inexpensive method for T_1 estimation when the T_R is unable to be held constant.

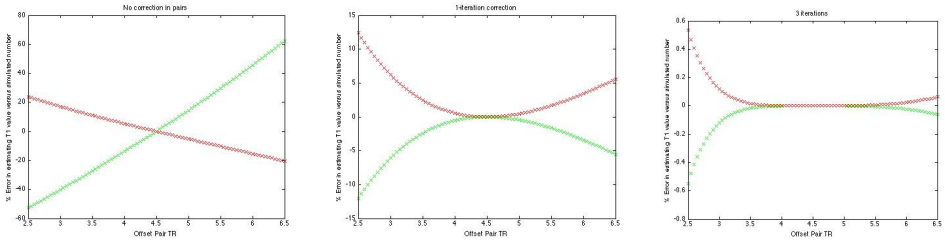

Figure 1. Error in T_1 (red) and M_0 (green) estimate in percent (y-axis) when base pairs have different TR value (x-axis). First base pair has TR held at 4.5ms and the second pair has the TR varied from 2.5ms to 6.5ms in 0.1ms increments (x-axis). **Left**: calculated directly without applying equation 6 assuming 'similar T_R value'. **Middle**: 1-iteration of equation 6. **Right** 3-iterations of equation 3.

When this method was applied to flow phantoms, we found similar results. However, when comparing values to DESPOT and IRSPGR estimated ground truth, it was found that our scanner had a gain of 1.6 relative to these

sequences. This highlights the need to run a calibration scan on a known flow phantom to determine gain prior to using estimated T_1 in for contrast agent estimation.

3.2 CA estimation

By calculating the uptake of contrast agent using Lo's method, we are able to quickly come up with an estimate within 1% of the Newton Raphson method for realistic values at a speed increase of over 100x. Equations 8 and 9 were used to generate intensity versus contrast agent concentration and plotted against each other in Figure 2.

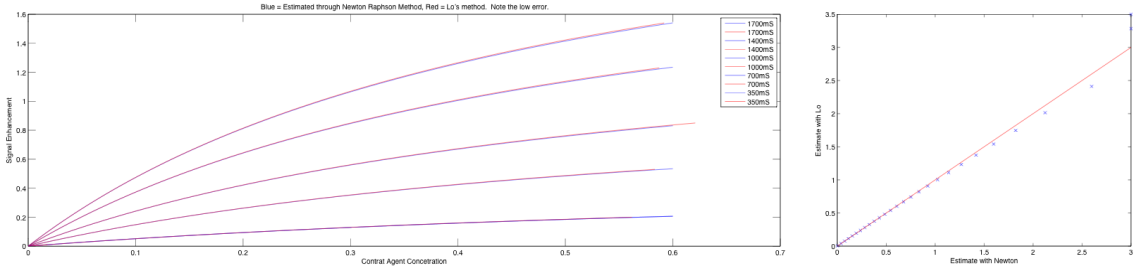

Figure 2. **Left**: CA concentration versus enhancement for various T_{10} values. Blue line estimate from Lo, red line estimate using Newton Raphson estimate, note that the near parity. **Right**: Newton estimate versus Lo estimate (blue x's), with the red line representing unity, note that for values less than 1500ms there is little variation.

3.3 PK Model correction methods

In our data various factors such as noise, start of uptake, and outliers played a large role in disrupting an accurate fit. Simulated data points were created and plotted in Figure 3 using equation 14 with the parameters [A,a,b] = [25,5.5,0.1], white noise was added, as was an outlier. As can be seen in when these factors are not considered, the estimated pharmacokinetic values can be impacted adversely with the original estimate (red) being [10,2.3,0.79], an error of 250%, while if the locus is detected and outlier eliminated the estimate is [28,6.1,0.091] or within 12%.

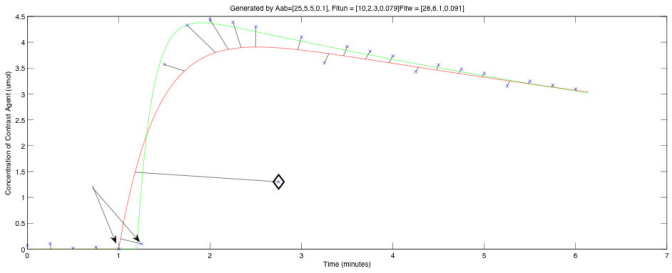

Figure 3 Blue 'x' generated from equation with added noise. Red line: direct. Black lines: nearest point. Green: curve fit with outlier deleted (black diamond) and origin shift (arrows). Green PK parameters within 15%, red > 200% off.

3.4 K^{trans} versus K^{trans} without optimizers

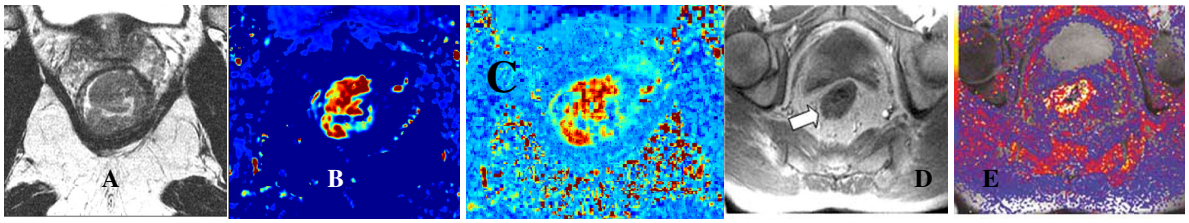

Figure 4. a) T_2W image b) K^{trans} using our method c) K^{trans} no correction, (d) T_2W image [7] (e) K^{trans} [7]

Figure 4 highlights the differences between our methodology and that commonly used for colorectal cancer trials. In this figure, 4A is a small field of view T_2 weighted image, and 4B is the K^{trans} calculated by our method. Figure

4C shows the K^{trans} calculated without using outliers, anisotropic filtering gating, or T_1 thresholding. When these two images are compared to the standard single-slice method used by Padhani [7] et al, the difference in contrast between regions is immediately noticed. In Padhani's image, 4E, the tumour shows only slightly more uptake than surrounding tissues, while we show that high transfer coefficients are isolated largely inside the cancerous region as would be expected. This is a similar result to that which occurs in our uncorrected estimation in Figure 4C.

3.5 Visualization of 3D PK parameters inside a medically segmented region of interest

When applying this methodology to a extract PK values from a 4D data set, the tumour can be visualized in 3D. To investigate the feasibility of using this methodology to delineate the boundaries of a tumour, and as a method to determine cancer spread we had a trained radiologist circle a region of interest marking radiologically cancerous regions on every slice through a 3D small field of view T2 weighted image (red). This region of interest was then compared to regions of high uptake on both A and K^{trans} (blue). These 3D regions were cropped and overlaid as shown in Figure 5. It is interesting to note the large amount of agreement between radiological cancerous regions and regions which are highlighted due to a large K^{trans} value. In these images, it shows that the region of interest marked by the radiologist is often larger than the region with a high uptake of contrast agent. Preliminary results show that this could be a tool to determine if the extent of spread has surpassed various surgical margins such as the circumferential resection margin.

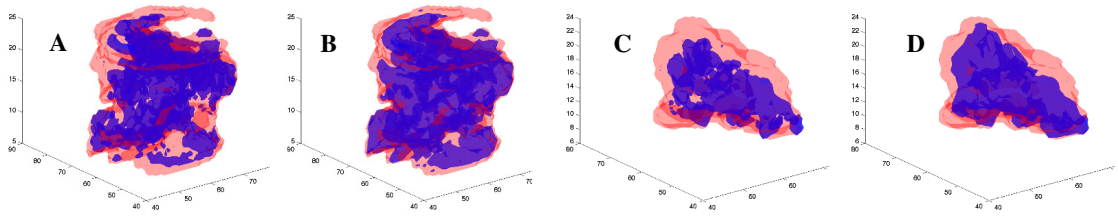

Figure 5. a) K^{trans} vs ROI b) A vs ROI, c) K^{trans} vs ROI d) A vs ROI. Note a,b & c,d are 2 different patients. Blue regions are where K^{trans} and A are above a threshold value.

4 Conclusion

In this paper we have outlined a very specific methodology that can be used for accurately and automatically estimating the pharmacokinetic values of 4D data sets. This type of analysis is quite useful in many types of cancer studies to determine transfer coefficients that could highlight information about a tumour that could then be used to select the proper treatment regime. Future work will continue to investigate these patients as they undergo chemoradiotherapy to see if there is a correlation between PK model variables and successful treatment outcome.

Acknowledgements

Project funded by NIHR Biomedical Research Centre Programme.

References

1. P. Armitage, C. Behrenbruch, J.M.Brady, and N. Moore, "Extracting and visualizing physiological parameters using dynamic contrast-enhanced magnetic resonance imaging of the breast," *Medical Image Analysis* vol. 9, pp. 315-329, 2005.
2. V. Chu, G. Hamarneh, "MATLAB-ITK Interface for Medical Image Filtering, Segmentation, and Registration", Proceedings of SPIE Medical Imaging: Image Processing, vol. 6144, 2006, pp. 1-8 (61443T-1 to 8).
3. S.C.L. Deoni, T.M. Peters, and B.K. Rutt, "High-Resolution T1 and T2 Mapping of the Brain in a Clinically Acceptable Time with DESPOT1 and DESPOT2," *Magnetic Resonance in Medicine*, vol. 53, pp. 237-241, 2005.
4. P.S. Tofts, B. Berkowitz, M.D. Schnall, "Quantitative analysis of dynamic Gd-DTPA enhancement in breast tumours using a permeability model." Magnetic Resonance in Medicine, 33(3), P564-8, 1995.
5. J.Lo, "Automated Breast Cancer Detection using Contrast-Enhanced MRI," in Engineering Science. vol. *DPhil Thesis: University of Oxford*, 2005.
6. P.S. Tofts, "Modeling tracer kinetics in dynamic Gd-DTPA MR imaging," *Journal of Magnetic Resonance Imaging*, vol. 7, pp. 91-101, 1997.
7. Atkin, N.J. Taylor, A.R. Padhani, plus et. al, "Dynamic contrast-enhanced magnetic resonance imaging is a poor measure of rectal cancer angiogenesis," *British Journal of Surgery*, vol. 93, 2006.